

# Towards detection of molecular parity violation by microwave spectroscopy of $\text{CpRe}(\text{CH}_3)(\text{CO})(\text{NO})$ \*\*

Nityananda Sahu,<sup>1</sup> Konstantin Gaul,<sup>1</sup>  
Anke Wilm,<sup>1</sup> Melanie Schnell<sup>2</sup> and Robert Berger<sup>1,\*</sup>

[<sup>1</sup>] Dr. Nityananda Sahu, Dr. Konstantin Gaul, Dr. Anke Wilm, Prof. Dr. Robert Berger

Fachbereich Chemie, Theoretische Chemie  
Philipps-Universität Marburg, Hans-Meerwein-Str. 4, 35032 Marburg, Germany

E-mail: robert.berger@uni-marburg.de

[<sup>2</sup>] Prof. Dr. Melanie Schnell

Deutsches Elektronen-Synchrotron DESY

Notkestr. 85, 22607 Hamburg, Germany

E-mail: melanie.schnell@desy.de

[\*\*] This work is financially supported by the Deutsche Forschungsgemeinschaft (DFG, German Research Foundation) – Projektnummer 328961117 – SFB 1319 ELCH. The center for scientific computing (CSC) Frankfurt is thanked for computer time.

May 9, 2023

*Parity-violating differences in rotational constants of a chiral 5d transition metal complex, that was previously experimentally well-characterised by broadband microwave spectroscopy, are predicted with a recently established efficient analytical derivative technique. Relative differences  $\Delta X/X$  between rotational constants  $X = A, B, C$  of enantiomers of the title compound are found to be on the order of  $10^{-14}$ , which is a favourably large effect. The quality of the theoretical estimates is carefully assessed by computing nuclear electric quadrupole coupling constants that agree well with experiment.*

One of the most intriguing effects of the fundamental weak force is that it can induce a tiny energy difference ( $\Delta E_{\text{pv}}$ ) between enantiomers of a chiral compound [1]. Although its existence has been predicted more than half a century ago [2, 3, 4], the parity-violating energy difference escaped all attempted measurements, despite its fundamental importance for our understanding of molecular chirality, its potential role in the evolution of biomolecular homochirality on planet earth [5, 6, 1]

and its use to probe specific candidates of dark matter [7, 8]. Early experimental approaches focused on vibrational spectroscopy, attempting to detect differences in the vibrational transition frequencies of enantiomers (see Fig. 1) [3, 9, 10, 11, 12].

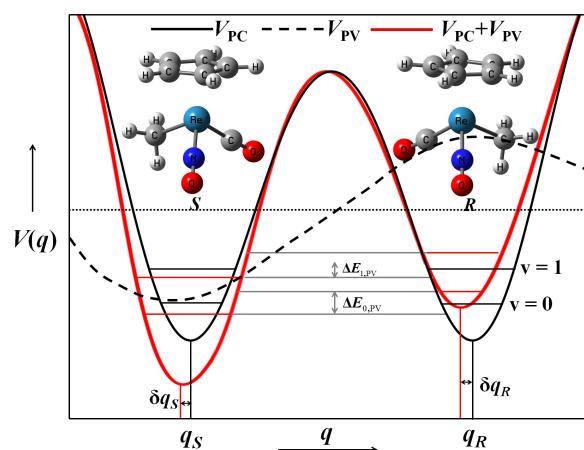


Figure 1: Parity conserving (pc) and parity-violating (pv) energy profile diagram for *S*- and *R*-enantiomers of the  $\text{CpRe}(\text{CH}_3)(\text{CO})(\text{NO})$  complex. Energies are not to scale and PV contributions are magnified by several orders of magnitude.

The currently tightest upper bound from experiment, provided for the splitting in the C–F stretch fundamental in  $\text{CHBrClF}$ , the prototypical chiral molecule [13, 14, 15], is on the order of  $\Delta v/v \approx 10^{-13}$  [16, 17]. This exceeds, however, the theoretically predicted splittings by about four orders of magnitude [18, 19, 20, 21, 22, 23, 24]. Compounds with heavier elements can, thus, become advantageous in this research line, because parity violating energy differences coarsely scale quintically with the nuclear charge  $Z$  of the heaviest elements. The single-center theorem [25] indicates that parity violating effects independent of the nuclear spin are suppressed in main group compounds with only a single heavy center, so that chiral methane derivatives with two heavy halogens like  $\text{CHAtFI}$  were proposed as a remedy [22]. Although such short-lived radioactive molecules were initially understood merely as theoretical toy models to explore limits in high- $Z$  regions, recent progress based on our theoretical laser-cooling proposal to explore parity violation *within the nucleus* of various isotopes of diatomic  $\text{RaF}$  [26] combined with the subsequent first laser-spectroscopic investigation of this short-lived molecule [27] changed the pic-

ture completely and initiated campaigns for molecular spectroscopy with radioisotopes at high-energy physics centers such as CERN near Geneva, FRIB in Michigan or TRIUMF in Vancouver to name but a few.

Another way to elegantly bypass the single-center theorem in chiral molecules is to turn to transition metal compounds, as their additional d-orbital involvement can produce comparatively large parity violating effects even in the absence of other heavy nuclei. Schwerdtfeger and coworkers thus searched for known chiral Re and Ir complexes and predicted their parity violating energy differences at the equilibrium structure of the electronic ground state to be comparatively large, on the order of 10 to 100 nJ mol<sup>-1</sup> (or 10<sup>-14</sup> E<sub>h</sub>) [28]. By virtue of Lethokov’s rule that relative parity violating energy splittings remain essentially the same in electronic, vibrational and rotational spectra [3], a Re complex and an Os complex with a double bond to O and C, respectively, to facilitate strong dipole transitions in the range of highly stable CO<sub>2</sub> lasers, were explored theoretically for large parity violating vibrational frequency splittings. And indeed, exceptionally large splittings of  $\Delta\nu/\nu = 10^{-14}$  were finally estimated [29].

While highly encouraging as a result, two obstacles severely hampered further progress for such complexes: 1) Ways to obtain enantiomerically enriched samples of the chiral molecules remained open and 2) nothing was known about the high-resolution gas phase spectroscopy of chiral transition metal complexes. But advances in microwave spectroscopy provided the solution to both: 1) Hirota’s microwave three-wave mixing proposal to selectively tag enantiomers of chiral molecules with C<sub>1</sub> symmetry [30] was successfully implemented experimentally [31] and makes spatial separation of enantiomers unnecessary. 2) Medcraft et al. reported the first high-resolution spectroscopy of racemic CpRe(CH<sub>3</sub>)(CO)(NO) and analysed the hyperfine-resolved rotational spectrum to obtain nuclear electric quadrupole coupling (NEQC) constants [32]. It was proposed before [33] that precision microwave spectroscopy of slowed chiral molecules might also be a promising route to detect parity-violating frequency splittings, although up to this date little is known about the magnitude of the corresponding line splittings in general and for transition metal compounds in particular. The reason is that parity-violation induced shifts in rotational constants in larger molecules are extremely tedious to predict as this requires, even in the most simple schemes, to compute gradients of parity violating potentials with respect to spatial displacements

of all the nuclei in the system. Thus, the rare predictions attempted so far concern light molecules with few atoms only like CHBrCIF ( $\Delta X/X \approx 10^{-17}$ ) [34] or fluorooxirane ( $\Delta X/X \approx 10^{-19}$ ) [35], for which these shifts were obtained with finite difference schemes in a one-component, non-relativistic framework [36]. Our most recent advances in theoretical approaches, however, allow such predictions for polyatomic heavy-elemental compounds via an efficient analytic gradient technique in a quasi-relativistic framework, and we have benchmarked this approach recently for CHBrCIF, CHClFI, CHBrFI and CHAtFI [23]. With this new approach, we are finally in the position to estimate rotational frequency splittings in transition metal complexes, most importantly the specific Re system analysed in high-resolution molecular spectroscopy by Schnell and coworkers [32].

CpRe(CH<sub>3</sub>)(CO)(NO) is quite interesting in several aspects: Firstly, the presence of both naturally occurring rhenium isotopes (<sup>187</sup>Re and <sup>185</sup>Re) and nitrogen (<sup>14</sup>N) with nuclear spins  $I \geq 1$  ( $I_{\text{Re}} = 5/2$  and  $I_{\text{N}} = 1$ ) leads to significant hyperfine structure in the spectrum. Secondly, the magnitudes of the nuclear quadrupole moments of the rhenium and nitrogen nuclei differ by more than two orders of magnitude. The magnitude of the hyperfine splitting reflects, besides the size of the electric quadrupole moment of the specific isotope, also the anisotropy in the electric-field gradient surrounding the quadrupolar nucleus, which can be used to describe the bonding situation in the vicinity of the respective nuclei. Thus, NEQC is sensitive to the electronic density in the vicinity of the nucleus, which is relevant for molecular parity violation, and thus having measurements of NEQC available allows to assess the quality of the theoretical description.

We consider herein the *R*-enantiomer of CpRe(CH<sub>3</sub>)(CO)(NO) for our study (*cf.* Fig. 2). Equilibrium rotational constants calculated with relativistic effective core potential (RECP) are listed in the Supporting Information and appear at first glance to be in reasonable agreement with experimentally observed values reported in Ref. [32]. On closer inspection, however, the RECP molecular structures obtained on the B3LYP level agree extremely well with regard to the measured *A* constant, but have smaller *B* and *C* constants because the cyclopentadienyl ring is found at too large a distance from the rhenium atom on this level. This structural feature impacts significantly on the computed NEQC constants in Cp<sup>187</sup>Re(CH<sub>3</sub>)(CO)(NO), for which we used a quasi-relativistic zeroth-order regular

approximation (ZORA) approach with different density functionals (ZORA-DFT) or within a Hartree–Fock framework (ZORA-HF) as described in Refs. [37, 38]. We compare to the NEQC tensor experimentally determined in Ref. [32] and study the influence of different density functionals on the energy optimization of the molecular structure as well as on molecular electronic density. A visualization of selected results for the NEQC tensor of  $^{187}\text{Re}$  in a polar tensor plot as suggested in Ref. [39] is shown in Fig. 2, whereas a complete list of results for the full NEQC tensors for  $^{187}\text{Re}$  and  $^{14}\text{N}$  at different levels of theory is provided in the Supplement. One can clearly see from Fig. 2 that HF gives rise to qualitatively wrong NEQC tensors both for the electronic density as well as for the molecular structure. Best results are received with hybrid functionals such as B3LYP and molecular structures optimized at the ZORA-DFT level. The difference between different functionals for computation of the electron density is comparatively small, in particular we observe that LDA agrees with B3LYP within 10% for the components of the NEQC tensor. This finding suggests that also for the prediction of PV effects in this chiral Re complex, results at the ZORA-DFT level are to be favoured over those from a HF treatment as the latter yields a qualitatively wrong description of the electron density close to the rhenium nucleus. To be specific for the parity conserving potentials, we use in the following the two-component ZORA-B3LYP equilibrium structure reported in Table S1 together with the corresponding harmonic vibrational force fields of Table S9 and S10. This structure provides on average the lowest deviations of the NEQC tensor from the experimental data, and various density functionals result in similar deviations, even when using the LDA functional.

After these benchmarks, we calculated with our two-component ZORA approach to electroweak quantum chemistry [41, 42, 43, 37, 23] the molecular PV energy  $E_{\text{PV}}^R$  of the  $R\text{-CpRe}(\text{CH}_3)(\text{CO})(\text{NO})$  enantiomer displayed on the right in Fig 1. For the ZORA-B3LYP as well as the RECP-B3LYP equilibrium structure, the values of  $E_{\text{PV}}^R$  for both of the isotopologues are of the order of  $10^{-9} \text{ cm}^{-1} hc$  (cf. Fig. 3). The difference of the PV potentials [ $\Delta E_{\text{PV}}^{R,S} = 2 \times E_{\text{PV}}^R$ ] between the  $R$ - and  $S$ -enantiomers is about  $3 \times 10^{-9} \text{ cm}^{-1} hc$  (ca. 90 Hz  $h$  or 40 nJ mol $^{-1}$ ). These effect sizes are comparable to previous predictions for other rhenium complexes [28, 29, 44]. The values of  $E_{\text{PV}}^R$  are seen to depend

on the choice of level of theory where both LDA and BLYP values are close to each other, deviating by about 1 % from each other, whereas B3LYP produces similar values and is numerically  $\approx 15\%$  larger than LDA and BLYP ones (see Supplementary Material). However, the HF  $E_{\text{PV}}^R$  value depends strongly on the molecular structure, being  $\approx 15\%$  larger than the LDA value for the RECP-B3LYP structure but  $\approx 15\%$  smaller than the LDA value for the ZORA-B3LYP structure

The experimental infrared spectrum of the complex shows two very strong signals at 1664 and 1932  $\text{cm}^{-1}$  [32], which correspond to the NO and CO stretching fundamentals, respectively. The gas-phase harmonic force field computed at the two-component ZORA-B3LYP level for  $R\text{-CpRe}(\text{CH}_3)(\text{CO})(\text{NO})$  for both of the  $^{187}\text{Re}$  (natural abundance 62.6 %) and  $^{185}\text{Re}$  (natural abundance 34.7 %) isotopologues give unscaled transition wavenumbers at 1791  $\text{cm}^{-1}$  for the NO stretch and 2032  $\text{cm}^{-1}$  for the CO stretch vibration. The variation of parity conserving (PC) and PV potentials as a function of the dimensionless reduced normal coordinate corresponding to CO and NO stretching modes of  $\text{Cp}^{187}\text{Re}(\text{CH}_3)(\text{CO})(\text{NO})$  are displayed in Fig. 3. The former potential is obtained at the two-component ZORA-B3LYP level, the latter is evaluated within a two-component ZORA-LDA approach. Cuts through PV potentials along the dimensionless reduced normal coordinates for other functionals like B3LYP and BLYP (see Supporting Information) follow similar patterns as that of LDA, whereas the plot due to HF is again different and deviates from the DFT methods, indicating, as already observed in Fig. 2, that HF results are unreliable for describing electronic properties of compounds containing transition metal centers. The LDA-slope of the PV potential in this two-dimensional vibrational manifold induces a tiny parity-violating change of the equilibrium structure leading to a shortened NO bond and an elongated CO bond of the  $R$ -enantiomer and vice versa for its mirror image.

The presence of non-zero PV energy gradients  $\vec{\nabla}E_{\text{PV}}$  at the minimum of the PC potential (cf. Tables S3-S4) leads, thus, to a change of the equilibrium structure of a chiral molecule. Inspired by the existing experimental broadband rotational spectrum of the  $\text{CpRe}(\text{CH}_3)(\text{CO})(\text{NO})$  complex [32], the analytically derived Cartesian PV energy gradients  $\vec{\nabla}E_{\text{PV}}$  are used to estimate the PV induced shifts of the equilibrium rotational constants. For the  $^{187}\text{Re}$  isotopologue, the values of  $\frac{\Delta X_{\text{R}}}{X_{\text{R}}}$  as obtained on the LDA level are displayed

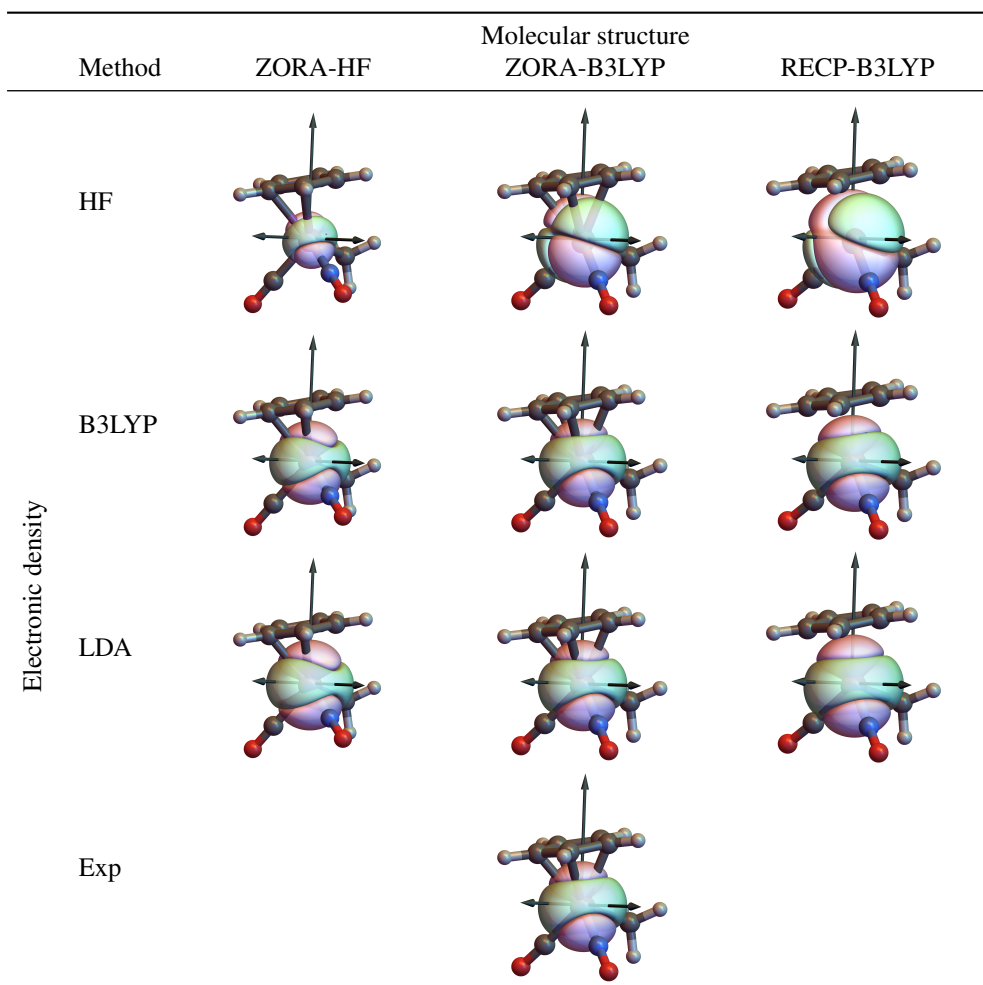


Figure 2: Visualization of nuclear electric quadrupole coupling tensors of  $^{187}\text{Re}$  in  $\text{Cp}^{187}\text{Re}(\text{CH}_3)(\text{CO})(\text{NO})$  with polar plots as described in Ref. [39]. Values for the corresponding experimental NEQC were taken from Ref. [32]. A nuclear electric quadrupole coupling constant of  $eQ = 207.0 \text{ fm}^2$  was used for  $^{187}\text{Re}$  as suggested in Ref. [40]. Molecules are aligned along the principal axes of rotation, which are shown as black arrows. Lengths of these arrows are scaled by the value of the corresponding rotational constant  $A, B, C$ .

in Fig. 3, other data can be located in the Supplementary Material. The relative shifts are favourably large, of the order of  $10^{-14}$  for all rotational constants. A similar magnitude but opposite signs were obtained for these on the HF level, but these latter values are to be discarded by virtue of the erroneous HF results for NEQCs in this compound.

Our explicit predictions for PV in rotational transitions of a 5d transition metal compound thus support Letokhov's rule of thumb for an overall consistency of relative PV effect sizes in rotational and vibrational

transitions. In vibrational transitions,  $\Delta\nu/\nu \approx 10^{-14}$  are projected to be resolvable with present day techniques for tailored experimental setups [45]. In rotational spectroscopy, however, the relative experimental resolution is presently lower for standard experiments, but here one can strongly benefit from a linear scaling of the splittings with rotational quantum number  $J$ , so that orders of magnitude can in principle be gained in high  $J$  transitions [18]. The resolution of a typical coaxial Fourier transform microwave spectroscopy experiment [46] employing a microwave resonator com-



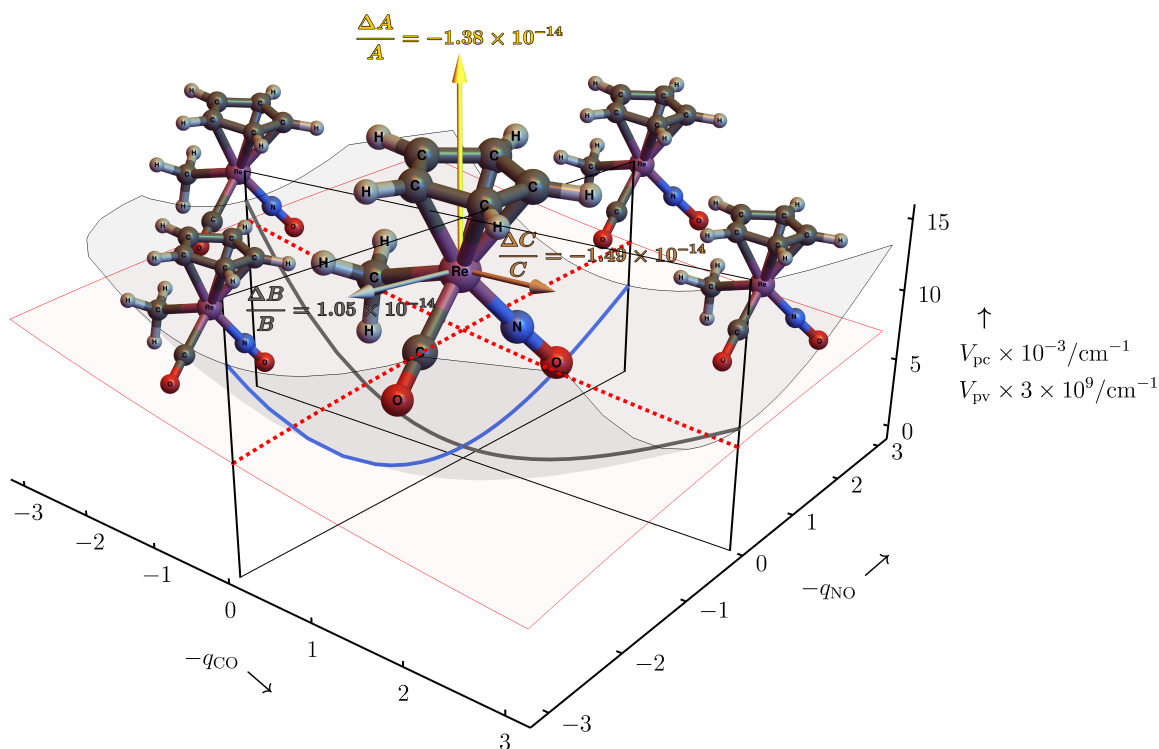


Figure 3: Visualization of parity violating shifts of the rotational constants of  $R\text{-Cp}^{187}\text{Re}(\text{CH}_3)(\text{CO})(\text{NO})$  as computed on the level of ZORA-LDA with the molecular structure optimized at the level of ZORA-B3LYP/x2c-TZVPPall-2c. The principal axes of rotation are shown in gold, silver and bronze with their length scaled by the value of the corresponding rotational constant  $A$ ,  $B$ ,  $C$  alongside their parity violating relative shifts  $\Delta A/A = -1.38 \times 10^{-14}$ ,  $\Delta B/B = 1.05 \times 10^{-14}$  and  $\Delta C/C = -1.49 \times 10^{-14}$ . The parity violating shifts of the rotational constants are proportional to the gradient of the parity violating potential at the equilibrium structure. The parity conserving potential  $V_{\text{pc}}$  is symbolically shown for the NO and CO stretching modes ( $q_{\text{NO}}$  and  $q_{\text{CO}}$ ) in the color of the involved atom (N blue and C gray). The parity violating potential is shown along these two modes as dotted red line. Surfaces that connect the cuts along  $q_{\text{NO}}$  and  $q_{\text{CO}}$  are shown to guide the eye but were not explicitly computed.

bined with supersonic expansion of the molecular sample is currently limited to 3–10 kHz ( $\approx 10^{-7}$  on the relative scale) depending on the carrier gas and thus on the velocity of the molecular beam due to mainly two reasons: i) the limited flight time of the molecules in the resonator and ii) the transverse motion of the molecules during the supersonic expansion accompanied by a significant loss of molecules from the area of high microwave field strength in the resonator [33]. The flight time can be increased significantly for example by elongating the resonator distance  $d$  and by using sources of translationally cold, decelerated molecules. For 20 m s $^{-1}$  slow molecules [47] and  $d = 1$  m, the molecules can be monitored up to 50 ms compared to 1 ms for non-decelerated beams using neon as a carrier gas (1000 m s $^{-1}$ ). [33] The resolution will be limited to 20–100 Hz Doppler broadening, but when measuring frequency differences between enantiomers in an alternating way, the resolving power of the experiment is not limited by the linewidth, but rather by the precision with which the frequency of the line centers can be determined. This is usually about one to two orders of magnitude better than the linewidths [48], so that the Hz range should be reachable. Furthermore, enantiomer-selective population transfer experiments based on advanced microwave pulse schemes can selectively populate or depopulate certain rotational states of interests by just changing the phase of one microwave pulse in the scheme, which can be highly advantageous for such experiments. [49, 50] Alternative approaches to perform microwave spectroscopy with perspective even higher resolution are Ramsey type arrangements using the method of separated oscillatory fields. [51]

We note in passing that we also attempted to predict parity violating wavenumber splittings in the CO and NO stretching fundamental using our recently described perturbative approach that uses finite differences of analytic PV potential gradients together with cubic parity conserving potentials to take multi-mode effects into account [23]. Although again relative PV splittings on the order of  $10^{-14}$  are obtained, which seem to be very reasonable estimates, the values change sign when multi-mode effects are accounted for. Due to near resonance conditions that also lead to significant IR intensity redistribution in the NO and CO stretching fundamental, a more detailed analysis of the coupling situation seems mandatory. Nevertheless, we report corresponding data as obtained for the slightly inferior RECP-B3LYP optimised structures and their (an)harmonic force fields in the Supplement for future

reference.

In summary, we were able to predict with our recently established quasi-relativistic methodology [23] the relative shifts in rotational constants that are induced by electroweak parity violation in the equilibrium structure of the heavy-elemental chiral complex CpRe(CH $_3$ )(CO)(NO) containing either  $^{187}\text{Re}$  or  $^{185}\text{Re}$  isotopes, for which a high-resolution gas-phase rotational spectrum has already been reported [32]. Analytically derived  $\vec{\nabla}E_{\text{PV}}$  have been utilised to predict large relative shifts of rotational constants of about  $10^{-14}$ . Due to pronounced barrier heights for internal rotation of the Cp and methyl groups, the chiral dynamics of CpRe(CH $_3$ )(CO)(NO) in the rovibronic ground state is expected to be dominated, similarly to S $_2$ Cl $_2$  [41, 52], by parity violating effects rather than tunnelling phenomena. The comparatively large PV effect in this compound is excellent news for experimental attempts to measure for the first time molecular parity violation in precision rotational spectroscopy of chiral molecules.

## Computational Details

Molecular structures were optimized at different levels of theory using the turbomole program package version 7.5[53] for non-relativistic calculations with a relativistic effective core potential (RECP) and a modified version [54] of the program package turbomole [55] for two-component ZORA calculations. Molecular structures were optimized at the level of DFT employing the PBE exchange-correlation functional [56], its hybrid version PBE0 [57] or the B3LYP exchange-correlation functional [58, 59, 60, 61] and on the level of HF. In RECP calculations, an Ahlrichs basis set of triple zeta quality with additional polarisation functions def2-TZVPP [62, 63] was used for all atoms or a correlation consistent Dunning basis set of quintuple zeta quality with additional polarisation functions cc-pV5Z for H, C, N and O together with a correlation consistent quadruple zeta basis set with core valence polarisation cc-pwCVQZ on Re. In both cases, an energy-consistent RECP of the Stuttgart group was employed for Re [64]. In two-component ZORA calculations a basis of triple zeta quality optimized for two-component all-electron calculations x2c-TZVPPall-2c was used.[65] Molecular structures were optimized until the norm of the cartesian gradient was below  $10^{-4} E_{\text{h}} a_0^{-1}$ .

For NEQC calculations, electronic densities were

optimized for all molecular structures on the two-component ZORA level with the x2c-TZVPPall-2c basis on H, C, N and O and an even-tempered basis set with 25 s, 25 p, 14 d, 11 f and 3 g functions on Re. The parameters of the even-tempered series are composed as  $\alpha_i = \gamma \beta_N^{N-i}$ ,  $i = 1, \dots, N$ , with  $N = 26$ ,  $\gamma = 0.02$  and  $\alpha_1 = 500000000$ , where exponents  $\alpha_{1-25}$  were used for s functions, exponents  $\alpha_{2-26}$  were used for p functions, exponents  $\alpha_{12-25}$  were used for d functions, exponents  $\alpha_{15-25}$  were used for f functions and exponents  $\alpha_{21-23}$  were used for g functions. All calculations were converged until energy changes between two successive iterations were smaller than  $10^{-9} E_h$ . Electronic densities were computed at the level of HF, PBE, PBE0 and B3LYP as well as with the DFT exchange-correlation functionals LDA[66, 60], BLYP[58, 59, 60] and BLYP.

For calculations of PV energies and PV gradients, electronic densities were optimized for the molecular structures on the level of RECP-B3LYP/cc-pV5Z,cc-pwCVQZ-PP (Ref. [32]) and ZORA-B3LYP/x2c-TZVPPall-2c, on the two-component ZORA level with the aug-cc-pVDZ basis set for hydrogen and the even-tempered basis set described above utilising for s and p functions, the exponents  $\alpha_{1-25}$  and  $\alpha_{2-26}$  and in the case of d functions  $\alpha_{20-24}$  for H, C, N and O atoms, and  $\alpha_{12-25}$  for the Re atom. Additionally, for Re f functions with exponents  $\alpha_{15-22}$  were used. PV energies and gradients were computed at the level of HF, B3LYP, BLYP and LDA. All calculations were converged until energy changes were smaller than  $10^{-9} E_h$  whereas the relative change of spin-orbit energy between two-successive iterations were dropped below  $10^{-13}$ . The threshold for neglecting of gradients of two-electron integrals was set to  $10^{-15} E_h a_0^{-1}$ .

In all two-component calculations of electronic densities and PV gradients, a normalized spherical Gaussian nuclear charge density distribution  $\rho_A(\vec{r}) = \frac{\zeta_A^{3/2}}{\pi^{3/2}} e^{-\zeta_A |\vec{r} - \vec{r}_A|^2}$  was used with  $\zeta_A = \frac{3}{2r_{\text{nuc},A}^2}$  and the root-mean-square radius  $r_{\text{nuc},A}$  was chosen as suggested by Visscher and Dyall [67]. Unless explicit isotopes are given, the nuclear mass number was determined as nearest integer to the relative atomic mass.

NEQC tensors and PV energies of two-component ZORA densities were computed using our toolbox approach [37]. Within this, NEQC tensors were computed as described in Ref. [38].

The analytically derived cartesian PV energy gradient  $\vec{\nabla} E_{\text{PV}}$  at the equilibrium structure of R-

CpRe(CH<sub>3</sub>)(CO)(NO) was computed as described in Ref. [23] and utilized for the estimation of the relative shifts of the rotational constants [18], which are in principle associated with the rotational transitions as described in Refs. [34, 23].

## References

- [1] R. Berger, J. Stohner, *Wiley Interdiscip. Rev.-Comput. Mol. Sci.* **2019**, *9*, e1396.
- [2] Y. Yamagata, *J. Theor. Biol.* **1966**, *11*, 495–498.
- [3] V. S. Letokhov, *Phys. Lett. A* **1975**, *53*, 275–276.
- [4] B. Y. Zel'dovich, D. B. Saakyan, I. I. Sobel'man, *JETP Lett.* **1977**, *25*, 94–97.
- [5] M. Quack, *Angew. Chem. Int. Ed.* **1989**, *28*, 571–586.
- [6] M. Quack, *Angew. Chem. Int. Ed.* **2002**, *41*, 4618–4630.
- [7] K. Gaul, M. G. Kozlov, T. A. Isaev, R. Berger, *Phys. Rev. Lett.* **2020**, *125*, 123004.
- [8] K. Gaul, M. G. Kozlov, T. A. Isaev, R. Berger, *Phys. Rev. A* **2020**, *102*, 032816.
- [9] O. N. Kompanets, A. R. Kukudzhanov, V. S. Letokhov, L. L. Gervits, *Opt. Commun.* **1976**, *19*, 414–416.
- [10] E. Arimondo, P. Glorieux, T. Oka, *Opt. Commun.* **1977**, *23*, 369–372.
- [11] A. Bauder, A. Beil, D. Luckhaus, F. Müller, M. Quack, *J. Chem. Phys.* **1997**, *106*, 7558–7570.
- [12] H. Hollenstein, D. Luckhaus, J. Pochert, M. Quack, G. Seyfang, *Angew. Chem. Int. Ed.* **1997**, *36*, 140–143.
- [13] J. Costante, L. Hecht, P. L. Polavarapu, A. Collet, L. D. Barron, *Angew. Chem. Int. Ed.* **1997**, *36*, 885–887.
- [14] M. Pitzer, M. Kunitski, A. Johnson, T. Jahnke, H. Sann, F. Sturm, L. Schmidt, H. Schmidt-Böcking, R. Dörner, J. Stohner, J. Kiedrowski, M. Reggelin, S. Marquardt, A. Schießler, R. Berger, M. Schöffler, *Science* **2013**, *341*, 1096–1100.

- [15] M. Pitzer, G. Kastirke, M. Kunitski, T. Jahnke, T. Bauer, C. Goihl, F. Trinter, C. Schober, K. Henrichs, J. Becht, S. Zeller, H. Gassert, M. Waitz, A. Kuhlins, H. Sann, F. Sturm, F. Wiegandt, R. Wallauer, L. P. H. Schmidt, A. S. Johnson, M. Mazenauer, B. Spenger, S. Marquardt, S. Marquardt, H. Schmidt-Böcking, J. Stohner, R. Dörner, M. Schöffler, R. Berger, *ChemPhysChem* **2016**, *17*, 2465–2472.
- [16] C. Daussy, T. Marrel, A. Amy-Klein, C. T. Nguyen, C. J. Bordé, C. Chardonnet, *Phys. Rev. Lett.* **1999**, *83*, 1554–1557.
- [17] M. Ziskind, C. Daussy, T. Marrel, C. Chardonnet, *Eur. Phys. J. D* **2002**, *20*, 219–225.
- [18] M. Quack, J. Stohner, *Phys. Rev. Lett.* **2000**, *84*, 3807–3810.
- [19] J. K. Laerdahl and P. Schwerdtfeger and H. M. Quiney, *Phys. Rev. Lett* **2000**, *84*, 3811–3814.
- [20] R. G. Vignone, R. Zanasi, P. Lazzeretti, A. Ligabue, *Phys. Rev. A* **2000**, *62*, 052516.
- [21] M. Quack, M. Willeke, *Helv. Chim. Acta* **2003**, *86*, 1641–1652.
- [22] R. Berger, J. L. Stuber, *Mol. Phys.* **2007**, *105*, 41–49.
- [23] S. A. Brueck, N. Sahu, K. Gaul, R. Berger, *arXiv:2102.09897 [physics.chem-ph]* **2021**.
- [24] G. Rauhut, P. Schwerdtfeger, *Phys. Rev. A* **2021**, *103*, 042819.
- [25] R. A. Hegstrom, D. W. Rein, P. G. H. Sandars, *J. Chem. Phys.* **1980**, *73*, 2329–2341.
- [26] T. A. Isaev, S. Hoekstra, R. Berger, *Phys. Rev. A* **2010**, *82*, 052521.
- [27] R. F. Garcia Ruiz, R. Berger, J. Billowes, C. L. Binnersley, M. L. Bissell, A. A. Breier, A. J. Brinson, K. Chrysalidis, T. E. Cocolios, B. S. Cooper, K. T. Flanagan, T. F. Giesen, R. P. de Groote, S. Franchoo, F. P. Gustafsson, T. A. Isaev, Á. Koszorús, G. Neyens, H. A. Perrett, C. M. Ricketts, S. Rothe, L. Schweikhard, A. R. Vernon, K. D. A. Wendt, F. Wienholtz, S. G. Wilkins, X. F. Yang, *Nature* **2020**, *581*, 396–400.
- [28] P. Schwerdtfeger, J. Gierlich, T. Bollwein, *Angew. Chem. Int. Ed.* **2003**, *42*, 1293–1296.
- [29] P. Schwerdtfeger, R. Bast, *J. Am. Chem. Soc.* **2004**, *126*, 1652–1653.
- [30] E. Hirota, *Proc. Jpn. Acad. Ser. B* **2012**, *88*, 120–128.
- [31] D. Patterson, M. Schnell, J. M. Doyle, *Nature* **2013**, *497*, 475–477.
- [32] C. Medcraft, R. Wolf, M. Schnell, *Angew. Chem. Int. Ed.* **2014**, *53*, 11656–11659.
- [33] M. Schnell, J. Küpper, *Faraday Disc.* **2011**, *150*, 33–49.
- [34] M. Quack, J. Stohner, *Z. Phys. Chem.* **2000**, *214*, 675–703.
- [35] R. Berger, M. Quack, J. Stohner, *Angew. Chem. Int. Ed.* **2001**, *40*, 1667–1670.
- [36] R. Berger, M. Quack, *J. Chem. Phys.* **2000**, *112*, 3148–3158.
- [37] K. Gaul, R. Berger, *J. Chem. Phys.* **2020**, *152*, 044101.
- [38] K. Gaul, R. Berger, *Mol. Phys.* **2020**, *118*, e1797199.
- [39] J. Autschbach, S. Zheng, R. W. Schurko, *Concepts Magn. Reson. Part A Bridg. Educ. Res.* **2010**, *36A*, 84–126.
- [40] P. Pyykkö, *Mol. Phys.* **2018**, *116*, 1328–1338.
- [41] R. Berger, N. Langermann, C. van Wüllen, *Phys. Rev. A* **2005**, *71*, 042105.
- [42] R. Berger, C. van Wüllen, *J. Chem. Phys.* **2005**, *122*, 134316.
- [43] S. Nahrwold, R. Berger, *J. Chem. Phys.* **2009**, *130*, 214101.
- [44] B. Darquie, C. Stoeffler, A. Shelkownikov, C. Daussy, A. Amy-Klein, C. Chardonnet, S. Zrig, L. Guy, J. Crassous, P. Souldard, P. Asselin, T. R. Huet, P. Schwerdtfeger, R. Bast, T. Saue, *Chirality* **2010**, *22*, 870–884.

- [45] A. Cournol, M. Manceau, M. Pierens, L. Lecordier, D. B. A. Tran, R. Santagata, B. Argence, A. Goncharov, O. Lopez, M. Abgrall, Y. L. Coq, R. L. Targat, H. A. Martinez, W. K. Lee, D. Xu, P. E. Pottie, R. J. Hendricks, T. E. Wall, J. M. Bieniewska, B. E. Sauer, M. R. Tarbutt, A. Amy-Klein, S. K. Tokunaga, B. Darquié, *Quantum Electron.* **2019**, *49*, 288–292.
- [46] J.-U. Grabow, E. S. Palmer, M. C. McCarthy, P. Thaddeus, *Rev. Sci. Instr.* **2005**, *76*, 093106.
- [47] S. Y. T. van de Meerakker, H. L. Bethlem, G. Meijer, *Nat. Phys.* **2008**, *4*, 595–602.
- [48] M. Quack, J. Stohner, M. Willeke, *Annu. Rev. Phys. Chem.* **2008**, *59*, 741–769.
- [49] S. Eibenberger, J. Doyle, D. Patterson, *Phys. Rev. Lett.* **2017**, *118*, 123002.
- [50] H. Singh, F. Berggötz, W. Sun, M. Schnell, *Angew. Chem. Int. Ed.* **2023**, e202219045.
- [51] A. J. de Nijs, W. Ubachs, H. L. Bethlem, *J. Mol. Spectrosc.* **2014**, *300*, 79–85.
- [52] N. Sahu, J. O. Richardson, R. Berger, *J. Comput. Chem.* **2021**, *42*, 210–221.
- [53] *TURBOMOLE V7.5 2020, a development of University of Karlsruhe and Forschungszentrum Karlsruhe GmbH, 1989-2007, TURBOMOLE GmbH, since 2007; available from <https://www.turbomole.org>.*
- [54] C. van Wüllen, *Z. Phys. Chem* **2010**, *224*, 413–426.
- [55] R. Ahlrichs, M. Bär, M. Häser, H. Horn, C. Kölmel, *Chem. Phys. Lett.* **1989**, *162*, 165–169.
- [56] J. P. Perdew, K. Burke, M. Ernzerhof, *Phys. Rev. Lett.* **1996**, *77*, 3865–3868.
- [57] C. Adamo, V. Barone, *J. Chem. Phys.* **1999**, *110*, 6158–6170.
- [58] A. D. Becke, *Phys. Rev. A* **1988**, *38*, 3098–3100.
- [59] C. Lee, W. Yang, R. G. Parr, *Phys. Rev. B* **1988**, *37*, 785–789.
- [60] S. H. Vosko, L. Wilk, M. Nuisar, *Can. J. Phys.* **1980**, *58*, 1200–1211.
- [61] A. D. Becke, *J. Chem. Phys.* **1993**, *98*, 1372–1377.
- [62] A. Schäfer, C. Huber, R. Ahlrichs, *J. Chem. Phys.* **1994**, *100*, 5829–5835.
- [63] F. Weigend, M. Häser, H. Patzelt, R. Ahlrichs, *Chem. Phys. Lett.* **1998**, *294*, 143–152.
- [64] D. Figgen, K. A. Peterson, M. Dolg, H. Stoll, *J. Chem. Phys.* **2009**, *130*, 164108.
- [65] P. Pollak, F. Weigend, *J. Chem. Theory Comput.* **2017**, *13*, 3696–3705.
- [66] J. C. Slater, *Phys. Rev.* **1951**, *81*, 385–390.
- [67] L. Visscher, K. G. Dyall, *At. Data Nucl. Data Tables* **1997**, *67*, 207–224.